Magnetization Measurement of a series of ribbons with composition of $Fe_{73.5-x}Cr_xCu_1Nb_3Si_{13.5}B_9$ alloys (x =1, 2, 3, 4, 5, 6, 7, 8, 9, 10, 12.5, 15 & 17.5) using a Superconducting Quantum Interface Device (SQUID) magnetometer

Md. Sultan Mahmud

*Professor of Physics and Head of the Department of Basic Sciences & Humanities,
University of Asia Pacific, 74/A, Green Road, Dhaka- 1215,
e-mail: head.bsh@uap-bd.edu*

Abstract:

There are various means of measuring magnetization of a substance. The magnetization of a substance is usually determined by measuring its magnetic moment divided by the volume or mass of the substance. In the present study magnetization has been measured using a Superconducting Quantum Interface Device (SQUID) magnetometer

Key Words: Magnetization, Magnetic Moment, Superconducting Quantum Interface Device (SQUID) Magnetometer

Introduction:

In the present work a Superconducting Quantum Interface Device (SQUID) magnetometer MPMS XL, USA was used for a detail study of the magnetic properties at the Department of Engineering Sciences, Angstrom Laboratory, Uppsala University, Sweden. The magnetic properties measurement system MPMS XL is a sophisticated analytical instrument configured specially for the study of the magnetic properties of small samples over a broad range of temperature from 4.2 K to 400 K and magnetic fields from –50 KOe to +50 KOe. This standard system made by Quantum Design Inc. USA can measure the magnetic moment of solid powder and liquid samples with a differential sensitivity of 10^{-9} emu and can handle a maximum signal size of 0.5 emu. A general view of the MPMS XL with its system components is shown in fig. 5.13. The most sensitive available device for measuring magnetic fields, based on this sensitive device the so-called 'SQUID magnetometers' have been

developed. SQUID magnetometers are used to characterize materials when the highest detection sensitivity over a broad temperature range and using applied magnetic fields up to several Tesla is needed. Nowadays, this instrument is widely used worldwide in research laboratories. The system is designed to measure the magnetic moment of a sample, from which the magnetization and magnetic susceptibility can be obtained. Therefore, SQUID magnetometers are versatile instruments that perform both, DC and AC magnetic moment measurement.
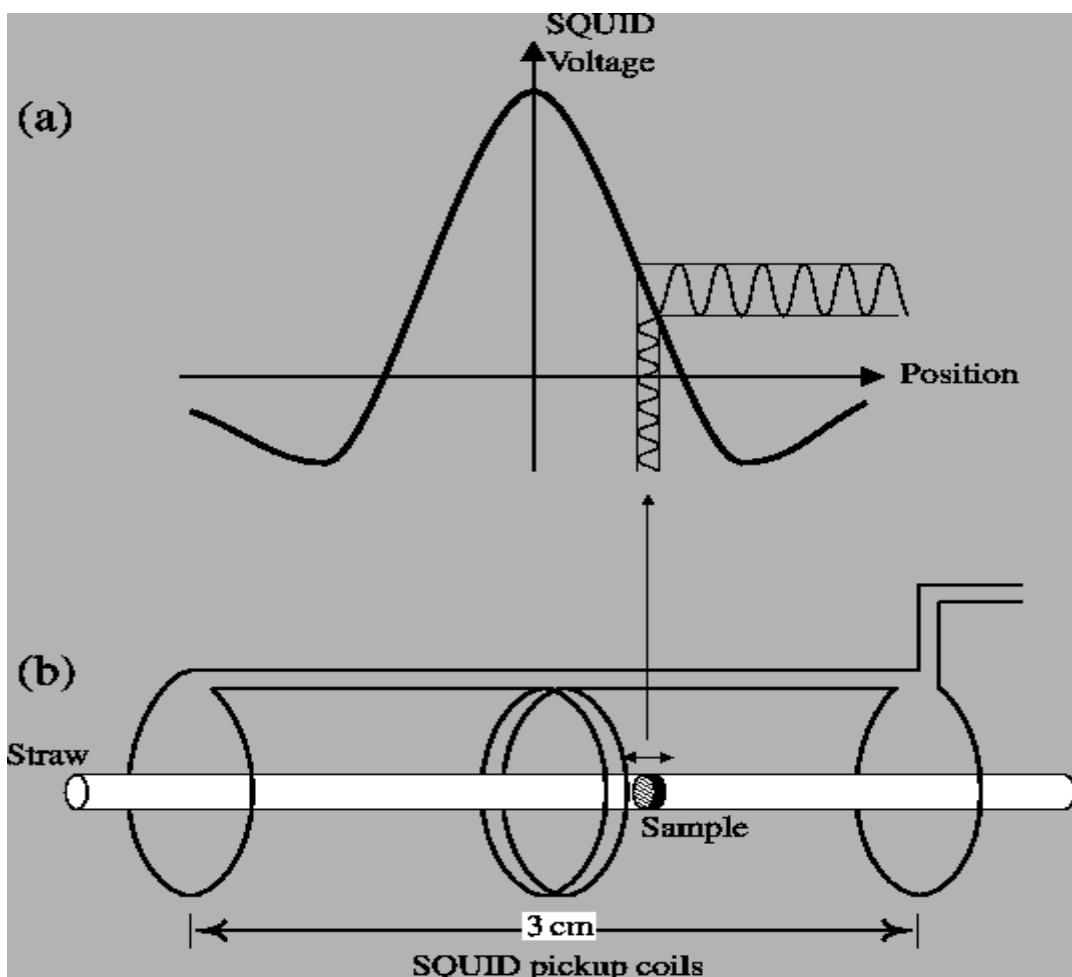

Fig. 1. SQUID Magnetometer.

The major components of a SQUID magnetometer are: superconducting magnet, superconducting detection coil, a SQUID connected to the detection coil, superconducting magnetic shield. Superconducting magnets are solenoid made of superconducting wire which must be kept at liquid helium dewar. The uniform magnetic field is produced along the axial cylindrical bore of the coil. The superconducting pick-up coil system, which is configured as a second order gradiometer is placed in the uniform magnetic field region of the solenoidal superconducting magnet. The SQUID device is usually a thin film that functions as an extremely sensitive current to voltage converter. Measurements are done in this equipment by moving the samples through the second order gradiometer. Hence, the magnetic moment of the sample induces an electric current in the pick-up coil system. Superconducting magnetic shield is used to shield the SQUID sensor from the fluctuations of the ambient magnetic field of the place where the magnetometer is located and from the large magnetic field produced by the superconducting magnet.

Using this kind of equipment we can measure the real and imaginary components of AC magnetic susceptibility as a function of frequency, temperature, AC magnetic field amplitude and DC magnetic field, and time. Using a specially designed sample holder the magnetic moment as a function of angle can also be measured.

It is an important feature of the instrument that one can change the magnetic field either by "oscillate mode" or "no overshoot mode". The oscillate mode is used to

minimize the remanent field of the magnet, whenever an accurate value of magnetic field is needed, e.g. in case of zero field cooling. In the hysteresis measurement the no overshoot mode has been selected, in which the field is changed directly from one value to another, and the magnet is returned to its persistent mode.

The MPMS XL features the new reciprocating sample measurement system. Unlike DC measurements where the sample is moved through the coils in discrete steps the RSO measurements are performed using a servomotor, which rapidly oscillates the sample is shown in fig.2.

A shaft encoder on the servomotor records the position of the sample synchronous with the SQUID signal. The data received is fitted to an ideal dipole moment response. To ensure this assumption is applicable samples need to be small: the calibration sample is a cylinder of 3 mm diameter and 3mm height. Sample of this size or smaller than an ideal point dipole to an accuracy of approximately 0.1%.

Figure 2. Illustration of an RSO measurement with small amplitude. (a) the ideal SQUID response for a dipole and (b) the movement of the sample within the SQUID pickup coils.

RSO measurements can be made in one of two configurations: Centre or maximum slope. Centre scans use large oscillations (2 or 3 cm) around the centre point of the pickup coils. These scans take a long time but the sample always remains properly located and a large number of measurements are recorded. These give the most accurate readings.

The maximum slope method oscillates the sample over a small region (0.2cm) at the most linear part of the SQUID response. The smaller amplitude makes measurements quicker and prevents the sample being subjected to significant magnetic field variation; however it also makes the measurement less accurate and susceptible to drift in the sample position.

The MPMS XL features significant improvements in the temperature control system. Utilizing a new design for the helium flow impedance, the MPMS XL has capability to operate continuously at temperatures below 4.2 K for indefinite periods of time- completely removing time limitations for making measurements in this temperature regime.

The new MPMS XL eliminates the operations associated with filling and recycling the He reservoir. Thus, the system solves the traditional problems of temperature instability and hysteresis associated with rapid boil off of liquid helium when warming through 4.2K. The results are smooth monotonic transitions across 4.2 K during both warming and cooling temperature sweeps. All these capabilities are fully automated for precise systems control and user-friendly operation.

The addition to a redesigned impedance system, the MPMS XL uses a new thermometer design for improved temperature accuracy and precise thermal control. The new thermometry, designed a developed at Quantum Design, is installed in close proximity to the sample within the sensitive coil detection region. The improved design is combined with new temperature control capabilities to provide more accurate measurements of the sample chamber, even under extreme temperature changes.

The new temperature sweep mode of operation provides MPMS XL users with the ability to take magnetic measurements while sweeping the system temperature at a controlled rate, automatically with no manual intervention. This mode provides a controlled, monotonic change in temperature during a measurement sequence at rates up to 10 K/min. Measurements of temperature dependence over large temperature ranges, which previously required time consuming temperature stabilization, can now be made quickly and precisely using temperature sweep mode.

Experimental:

A series of amorphous ribbons with composition of $Fe_{73.5-x}Cr_xCu_1Nb_3Si_{13.5}B_9$ alloys with x =1, 2, 3, 4, 5, 6, 7, 8, 9, 10, 12.5, 15 & 17.5 were prepared in an arc furnace on a water-cooled copper hearth under an atmosphere of pure Ar. Their purity and origin of the constituent elements were Fe (99.98%), Cu (99+%), B (99.5%), Si (99.9%), Nb (99.8%) and Cr (99.99%) as obtained from Johnson Mathey (Alfa Aesar Inc.) [1]. The required amounts of constituent elements were taken from pure metal bars or flakes weighed carefully with a sensitive electronic balance and placed on the copper hearth

inside the arc furnace. Before melting the furnace chamber was evacuated (10^{-4} torr) and flashed with Ar gas. The process was repeated several times to get rid of residual air and finally the furnace chamber was kept in an Ar atmosphere.

Fig.3. Vacuum arc melting machine

A substantial amount of pure Titanium getter, placed inside of the chamber on the side of the copper hearth was melted first in order to absorb any oxygen present in the furnace chamber. The constituent elements were then melted in the shape of buttons. The arc melting facilities used to prepare the samples are installed at the Centre for Materials Science, National University of Hanoi, Vietnam. The arc furnace used in the preparation of master alloys is shown in 3.
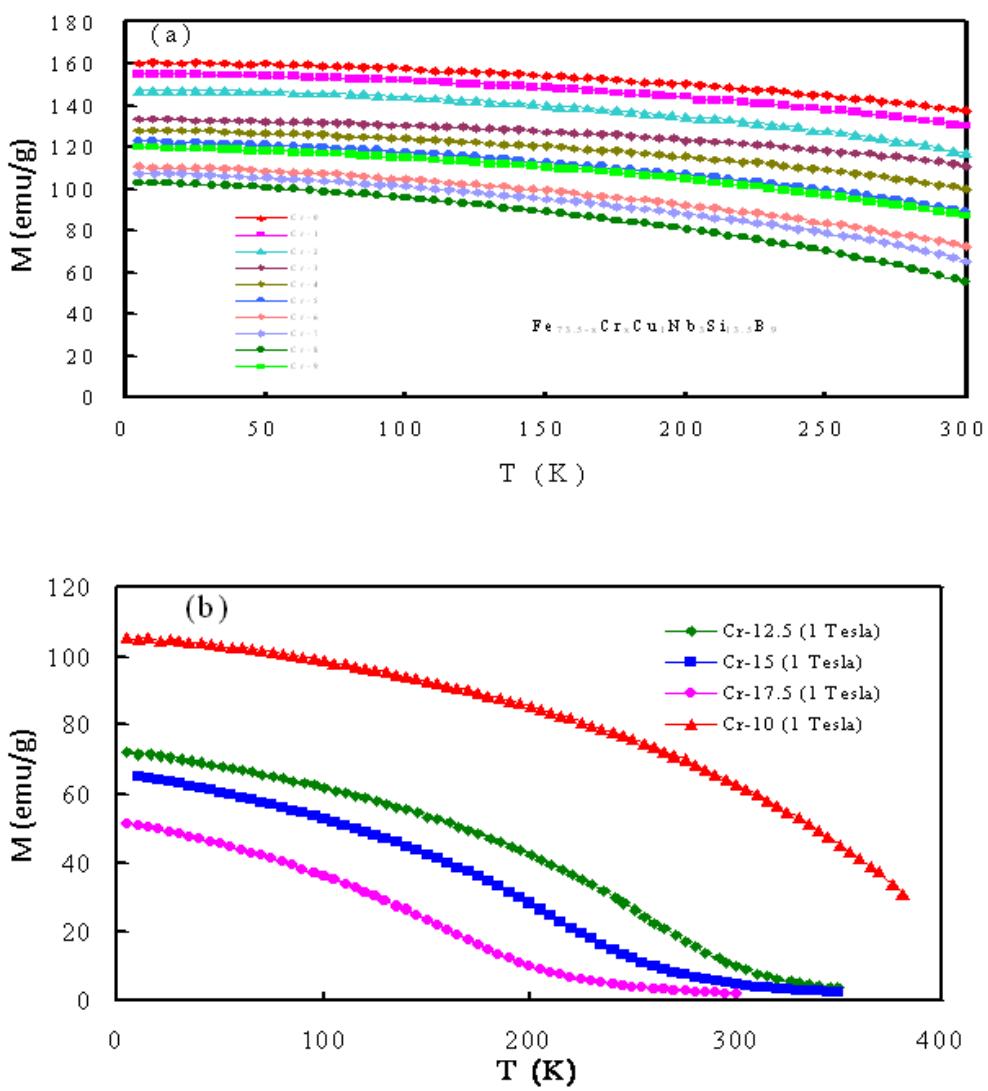
Results & Discussions:

It is well known that metallic glasses (amorphous) exhibit spin wave excitation [2,3,5] The alloys under study are FINEMET type of amorphous alloys with composition $Fe_{73.5-x}Cr_xCu_1Nb_3Si_{13.5}B_9$ (x = 0, 1, 2, 3, 4, 5, 6, 7, 8, 9, 10, 12.5, 15 & 17.5) in the as-prepared condition. In order to verify whether these alloys also exhibit spin wave excitation, the low temperature magnetization measurement as a function of temperature from 5K to 300K with an applied magnetic field of 1 Tesla has been carried out [4]. The experimental behavior of the saturation magnetization at low temperature was found to follow the Bloch's spin-wave theory according to the following equation [6-7]:

$$M(T) = M_0(1 - BT^{\frac{3}{2}} - CT^{\frac{5}{2}}) \qquad\qquad\qquad (1)$$

where M_0 is the saturation magnetization extrapolated at 0 K, B & C are the constants. Generally, the low temperature behavior of the saturation magnetization of crystalline ferromagnetic materials can be described within reasonable errors by the first two terms of equation (1) covering narrow range of temperature i.e. 0.2 T_c [8].

Fig. 4 (a, b) shows the temperature dependence of magnetization from 5K to 300K for all the samples. It is observed that the magnetization relaxes gradually with the increase of the Cr content and temperature.

Fig. 4 Temperature dependence of magnetization of amorphous $Fe_{73.5-x}Cr_xCu_1Nb_3Si_{13.5}B_9$ ribbons with an applied field 1 Tesla for (a) $0 \leq x \leq 9$ and (b) $10 \leq x \leq 17.5$

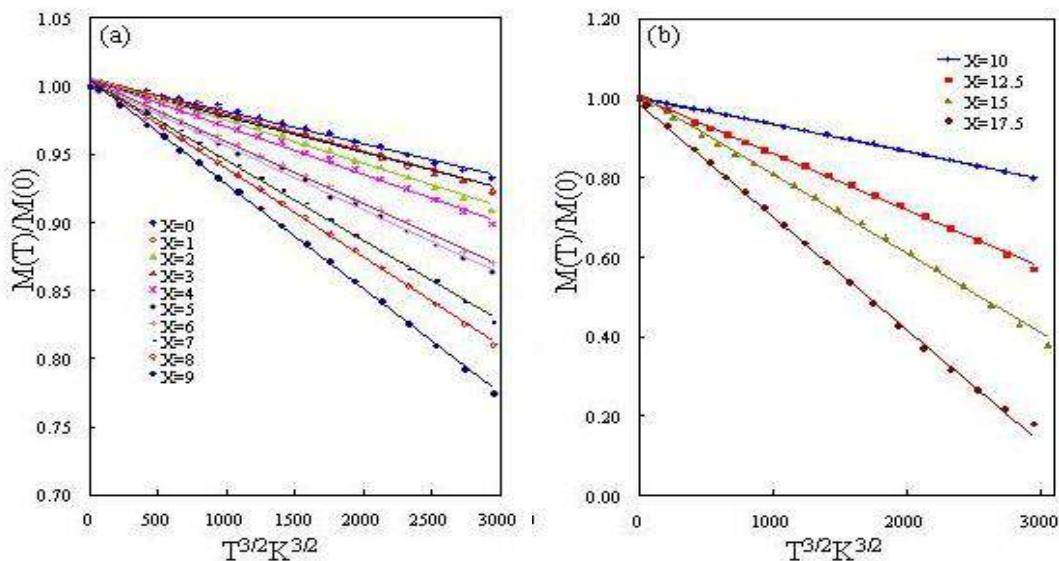However, inclusion of higher temperature term $T^{\frac{5}{2}}$ of the equation (1) an attempt has been taken to fit the experimental data of M(T) up to $0.6 \leq \dfrac{T}{T_c} \leq 0.8$ for all the samples which show also quite good fitting as shown in Fig. 6 (a, b) using the relation

$$\frac{\Delta M}{M_0} = \frac{M_0 - M(T)}{M_0} = BT^{\frac{3}{2}} + CT^{\frac{5}{2}} \tag{2}$$
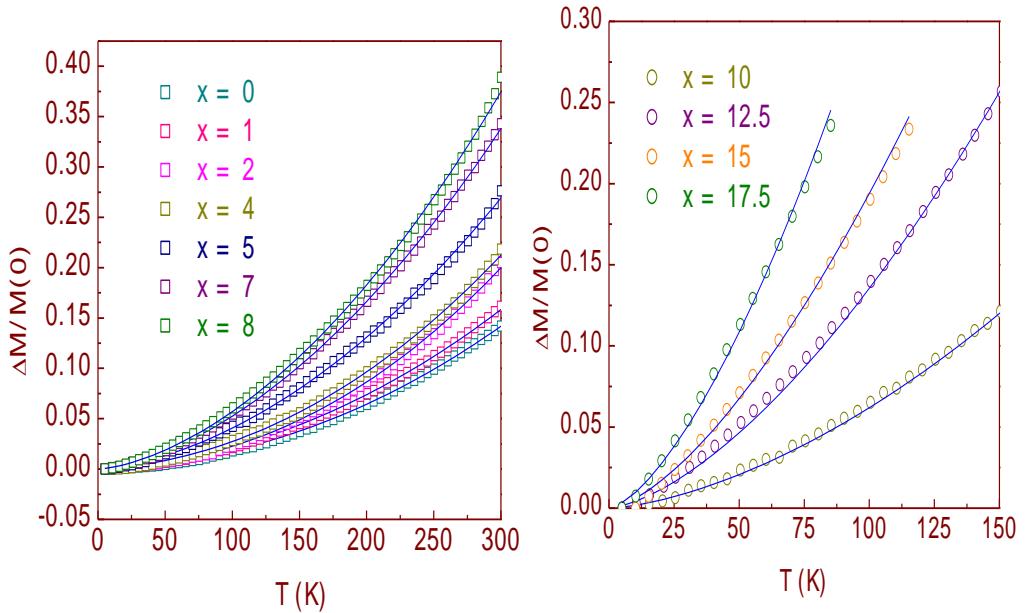
This indicates that the contribution to magnetization in this temperature range is from low and high-energy spin density waves.

The values of the coefficients B determined from the curves in fig. 5 have been used to fit the nonlinear curves in fig.6 (a, b) considering the high temperature term $T^{5/2}$ by adjusting the value of B and C for best fitting. The spin wave stiffness constant D and the mean square value of the range of exchange interaction $<r^2>$ was calculated [3].
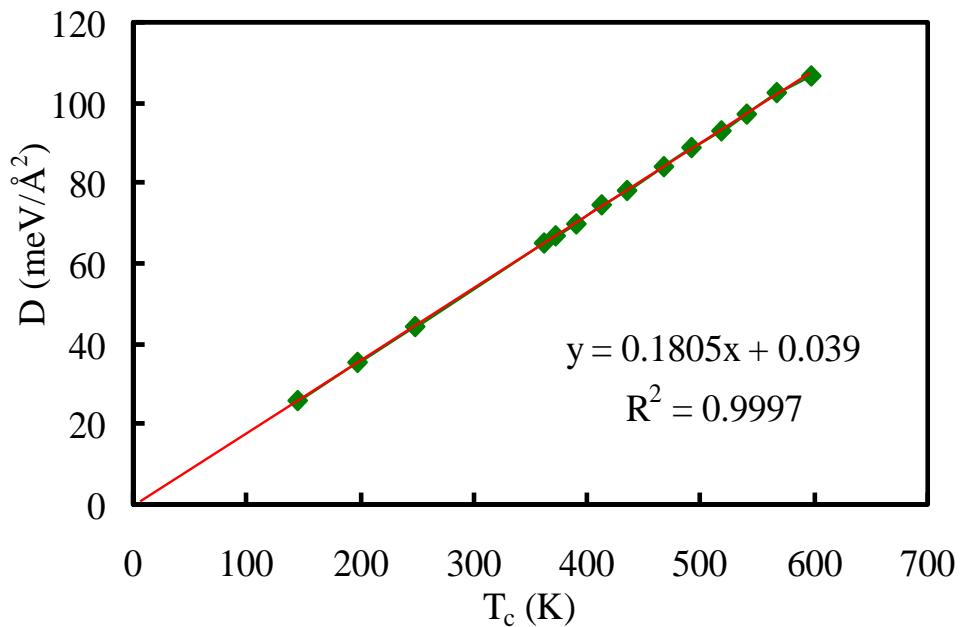
The values of the coefficient B, C, spin-wave stiffness constant D, the mean square value of the range of exchange interactions $<r^2>$, $\dfrac{C}{B}$ ratio and M_0 are shown in table-1 together with the value of crystalline Fe.

Fig. 5 The dependence of reduced magnetization $\dfrac{M(T)}{M(O)}$ **as a function of** $T^{\frac{3}{2}}$ **of amorphous ribbons with composition Fe$_{73.5-x}$Cr$_x$Cu$_1$Nb$_3$Si$_{13.5}$B$_9$ (a) x = 0, 1, 2, 3, 4, 5, 6, 7, 8 & 9 and (b) x = 10, 12.5, 15 & 17.5 Symbol: Experimental data and full line fitted with the equation (1)**

Fig. 6 Fitting of the low temperature magnetization data with the equation (7) in the temperature range (a) (5-300K) for $0 \leq x \leq 8$ and (b) 5-250K for $10 \leq x \leq 17.5$ for the amorphous Fe$_{73.5-x}$Cr$_x$Cu$_1$Nb$_3$Si$_{13.5}$B$_9$ ribbons

Fig. 7 Spin wave stiffness constant (D) as a function of Curie temperature (T$_C$)

Table-1 parameters describing the temperature dependence of magnetization of the amorphous ribbons with composition $Fe_{73.5-x}Cr_xCu_1Nb_3Si_{13.5}B_9$

Cr content x at.%	B ($K^{-3/2}$)	C($K^{-5/2}$)	C/B (K^{-1})	M(O) emu/g at 0 K	D_{SP} meV $Å^2$	$<r^2>$ $Å^2$	Temp. range of fitting
0	18.3×10^{-6}	3.85×10^{-8}	2.10×10^{-3}	160.3	107	27.0	$0< T/T_C<0.6$
1	20.0×10^{-6}	4.10×10^{-8}	2.05×10^{-3}	155.3	103	25.4	$0< T/T_C<0.6$
2	22.7×10^{-6}	4.62×10^{-8}	2.04×10^{-3}	147.6	98	24.0	$0< T/T_C<0.6$
3	27.0×10^{-6}	5.02×10^{-8}	1.86×10^{-3}	133.4	93	21.0	$0< T/T_C<0.6$
4	30.0×10^{-6}	5.50×10^{-8}	1.83×10^{-3}	127.8	89	20.0	$0< T/T_C<0.7$
5	34.0×10^{-6}	6.00×10^{-8}	1.76×10^{-3}	122.9	84	18.0	$0< T/T_C<0.7$
6	39.0×10^{-6}	6.30×10^{-8}	1.62×10^{-3}	119.7	78	15.2	$0< T/T_C<0.7$
7	45.0×10^{-6}	6.25×10^{-8}	1.39×10^{-3}	111.2	75	12.5	$0< T/T_C<0.8$
8	51.0×10^{-6}	6.80×10^{-8}	1.33×10^{-3}	107.8	70	11.2	$0< T/T_C<0.8$
9	57.0×10^{-6}	7.32×10^{-8}	1.28×10^{-3}	103.1	67	10.3	$0< T/T_C<0.8$
10	58.0×10^{-6}	6.80×10^{-8}	1.17×10^{-3}	92.8	65	9.2	$0< T/T_C<0.8$
12.5	152.0×10^{-6}	15.00×10^{-8}	0.987×10^{-3}	72.6	44	5.3	$0< T/T_C<0.8$
15	234.0×10^{-6}	6.50×10^{-8}	0.278×10^{-3}	67.2	35	1.2	$0< T/T_C<0.6$
17.5	480.0×10^{-6}	12.00×10^{-8}	0.250×10^{-3}	52.8	26	0.8	$0< T/T_C<0.6$
Fe	3.4×10^{-6}	0.10×10^{-8}	0.294×10^{-3}	220	286	$16a^2$	-

It is observed that the values of B, C for the studied samples increases gradually as the Cr content is increased. These values are much larger than the crystalline Fe, which is characteristic of amorphous ferromagnet [7,9]. The mean-square value of the range of exchange interaction $<r^2>$, decreases gradually with the increase of Cr content having a value of 27 $Å^2$ for x = 0 to 0.8 $Å^2$ for x = 17.5. These values are much smaller than that of crystalline ferromagnet. The low value of $<r^2>$ as compared with the Fe indicates that the range of exchange interaction is shorter in the Finemet type of amorphous alloys in comparison with that in crystalline ferromagnets in agreement with the previously published reports [6, 9,16]. The values of spin-wave stiffness constant (D) decreases monotonically from 107 meV $Å^2$ for x = 0 to 26 meV $Å^2$ for the sample x = 17.5. These values are much lower than crystalline Fe, which is 286 meV $Å^2$. The smaller values of spin-wave stiffness constant (D) in the studied system is an indication of the softening of the exchange interaction according to Varga *et al.* [7]. Our experimental values of D are very typical for amorphous materials and agree reasonably well with the values reported earlier in the literature [14, 7, 9, 11, 13]. The $\frac{D}{T_c}$ for the amorphous ferromagnets is generally smaller in comparison to the value of 0.27 for crystalline Fe which is indicative of the short-range nature of interactions in our studied system [7, 10, 12]. Our experimental $\frac{D}{T_c}$ = 0.18 for the whole series of alloys which corresponds well with the value of $\frac{D}{T_c}$ = 0.21 [14], 0.18 [12] for the amorphous alloys. The reduction in the value of D with the substitution of Fe by Cr

may be interpreted as due to an increase in the distance between Fe atoms. This leads to the weakening of exchange interaction between Fe atoms resulting in the lowering of Curie temperature [17]. Fig. 7 shows the exchange stiffness constant D, as a function of T_c. A linear dependence of D with T_c is observed for the entire composition range, which passes through the origin. The value of $\dfrac{D}{T_c} = 0.18$ remains constant (table-1) for all the compositions studied which indicates that the range of exchange interaction is not modified when Fe is substituted by Cr.

Conclusion:

The temperature dependence of magnetization of all the amorphous $Fe_{73.5-x}Cr_xCu_1Nb_3Si_{13.5}B_9$ (0 ≤x ≤17.5) alloys apparently follows the predictions of Bloch's Spin-wave theory including $T^{5/2}$ term in the temperature range $0.6 \leq \dfrac{T}{T_c} \leq 0.8$. The mean-square value of the range of exchange interaction $<r^2>$ and the values of spin-wave stiffness constant (D) decreases monotonically with the increase of Cr content. The values of $<r^2>$ are much smaller than that of crystalline ferromagnet implying that the range of exchange interaction is shorter in amorphous alloys. The smaller values of D in the studied system indicate weakening of the exchange interaction due to an increase in the distance between Fe atoms as the substitution of Fe by Cr occurs.

A linear dependence of D with T_c is observed for the entire composition range, which passes through the origin. The $\dfrac{D}{T_c} = 0.18$ has been determined from the slope of the straight line which is much smaller than the crystalline Fe $\left(\dfrac{D}{T_c} = 0.27 \right)$ and gives further indication regarding the short range nature of interaction in our studied amorphous system as expected.

References:

[1]   Md.Sultan Mahmud, International Journal of Advanced Materials Science, Vol. 5, No. 1 (2014) 5-11.
[2]   C. L. Chien, and R. Hasegawa, Phys. Rev. B16, 2115 (1977)
[3]   K. Handrich, S. Kobe, Amorphe Ferro and Ferrimagnetica, Akademie- Verlag Berlin, Germany (1980)
[4]   Md.Sultan Mahmud, International Journal of Advanced Materials Science, Vol. 5, No. 1 (2014) 61-67.
[5]   N. Ponpandian, A. Narayanasamy, K. Chattopadhyay and M. Manivel Raja, J. Appl. Phys. 93, No. 10, 6182 (2003)
[6]   S. M. Bhagat, M. L. Spano and K. V. Rao, J. Appl. Phys. 50(3), 1580 (1979)
[7]   S. N. Kaul, Phus. Rev. B 24(11), 6550 (1981)

[8]   <u>Md.Sultan Mahmud,</u> Journal of Materials Science and Engineering A1 (2011) 58-63.

[9]   S. Ramasamy, Leif Lundgren, K Ganesan and A Narayanasamy, J. Phys. F: Met. Phys. 17, 753-765 (1987)

[10]   L. K. Varga, F. Mazaleyrat, J. Kovac, and A. Kakay, Mat. Sci. Engg. A, 304-306, 946 (2000)

[11]   E. Pulido, P. Crespo and Hernando, IEEE Transactions on Magnetics, 28, 3189 (1992)

[12]   D. Prabhu, A. Narayanasamy, K. Chattopadhay, Journal of Non-Crystalline Solids, 353, 1577-1581 (2007)

[13]   Kyeong-Sup Kim, Seong-Cho Yu, Suhk-Kum Oh, Yong-Soocho, Taik-Kee Kim, JMMM 133, 283-286 (1994)

[14]   K. S. Kim, S. C. Yu, K. Y. Kim, T. H. Noh and I. K. Kang, IEEE Trans. Magn. 29, 2679 (1993)

[15]   R.Krishnan, M.Dancygier, M.Tarhouni., J.Appl.Phys.,63,7768 (1982)

[16]   <u>Md. Sultan Mahmud,</u> Asian Transactions on Science & Technology 1(3) (2011) 1-6.

[17]   M.A.Hakim, S.S.Sikder, <u>Md. Sultan Mahmud,</u> S.Manjura Hoque, P.Nordblad, Journal of the Korean Physical Sciences (JKPS) 53(2) (2008) 766-771